Journal of Medicinal Chemistry

Article

pubs.acs.org/jmc

Synthesis, Biological Evaluation, And Molecular Modeling of Chalcone Derivatives As Potent Inhibitors of *Mycobacterium tuberculosis* Protein Tyrosine Phosphatases (PtpA and PtpB)

Louise Domeneghini Chiaradia,[†,‡] Priscila Graziela Alves Martins,[†] Marlon Norberto Sechini Cordeiro,[‡] Rafael Victorio Carvalho Guido,[§] Gabriela Ecco,[†] Adriano Defini Andricopulo,[§] Rosendo Augusto Yunes,[‡] Javier Vernal,[†] Ricardo José Nunes,*[,‡] and Hernán Terenzi*[,†]

[†]Centro de Biologia Molecular Estrutural, CEBIME−UFSC, Universidade Federal de Santa Catarina, Campus Trindade, 88040−900 Florianópolis−SC, Brasil

[‡]Laboratório Estrutura e Atividade, Departamento de Química, LEAT−CFM−UFSC, Universidade Federal de Santa Catarina, Campus Trindade, 88040−900 Florianópolis−SC, Brasil

[§]Laboratório de Química Medicinal e Computacional, Instituto de Física de São Carlos, Universidade de São Paulo, Av. Trabalhador São-Carlense 400, 13560−970 São Carlos−SP, Brasil.

Supporting Information

ABSTRACT: Tuberculosis (TB) is a major infectious disease caused by *Mycobacterium tuberculosis* (Mtb). According to the World Health Organization (WHO), about 1.8 million people die from TB and 10 million new cases are recorded each year. Recently, a new series of naphthylchalcones has been identified as inhibitors of Mtb protein tyrosine phosphatases (PTPs). In this work, 100 chalcones were designed, synthesized, and investigated for their inhibitory properties against MtbPtps. Structure−activity relationships (SAR) were developed, leading to the discovery of new potent inhibitors with IC_{50} values in the low-micromolar range. Kinetic studies revealed competitive inhibition and high selectivity toward the Mtb enzymes. Molecular modeling investigations were carried out with the aim of revealing the most relevant structural requirements underlying the binding affinity and selectivity of this series of inhibitors as potential anti-TB drugs.

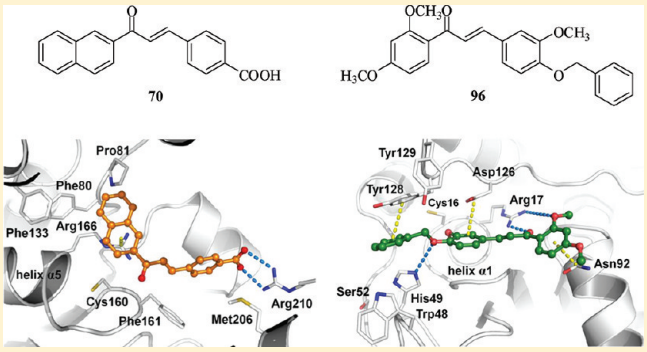

1. INTRODUCTION

Tuberculosis (TB) is an important disease due to infection by *Mycobacterium tuberculosis* (Mtb) which primarily affects the respiratory tract. According to the World Health Organization (WHO), there are nearly 10 million new cases of TB and 1.8 million deaths each year. The situation is further worsened by the co-infection with HIV due to the devastating effects of Mtb on the vulnerable immune system of the patients.[1] Despite BCG vaccine (Bacillus Calmette−Guerin) and the combined chemotherapy with first-line (isoniazid, ethambutol, rifampicin, pyrazinamide) or second-line (ethionamide) antibiotics (WHO), Mtb is the agent which causes more deaths from infection in the world. The chemotherapy involves the use of these four antibiotics for 6−9 months, resulting in significant lack of patient adherence to long-term therapy. The global emergence of multidrug-resistant (MDR) strains of Mtb is also a serious health problem.[2] For these reasons, there is an urgent need for new safe and effective anti-TB drugs.

The protein tyrosine-phosphatases (PTPs) are a family of regulatory enzymes that are closely related, and together with protein tyrosine kinases (Ptks) have a key role in the control of the phosphorylation state of tyrosines in the cells. The interaction between these two classes of enzymes is crucial to control the phosphorylation/dephosphorylation cascades, which are involved in several cellular processes.[3] On the basis of the Mtb genome, it was possible to identify two phosphotyrosine phosphatase genes, MtbPtpA and MtbPtpB.[4] While PtpA is classified as a low-molecular-weight protein (LMW PTP),[5] which specifically dephosphorylates tyrosine residues,[6] PtpB is a phosphatase with triple specificity (TSP PTP), which catalyzes the dephosphorylation of both residues (serine/threonine or tyrosine) and also has phosphoinositide phosphatase activity.[7,8] The enzymes PtpA and PtpB are secreted by Mtb into the host cell and attenuate host immune defenses by interfering with the host signaling pathways.[9−11] Confirming this fact, it was identified in macrophages the vacuolar protein sorting 33 homologue B (VPS33B), a

Received: September 20, 2011
Published: December 2, 2011

 © 2011 American Chemical Society

Scheme 1. Synthesis of Chalcone Derivatives 1−47[a]

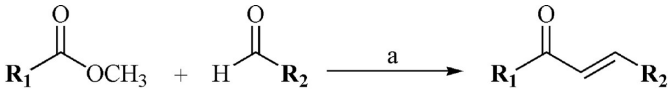

1-47

Comp	R_1	R_2	Comp	R_1	R_2
1	3,4-methylenedioxy-Ph	4-Cl-Ph	**2***	3,4-methylenedioxy-Ph	3-Cl-Ph
3	3,4-methylenedioxy-Ph	2,6-Cl_2-Ph	**4***	3,4-methylenedioxy-Ph	3,4-Cl_2-Ph
5	3,4-methylenedioxy-Ph	4-NO_2-Ph	**6**	3,4-methylenedioxy-Ph	3-NO_2-Ph
7	3,4-methylenedioxy-Ph	4-Br-Ph	**8**	3,4-methylenedioxy-Ph	4-OCH_3-Ph
9	3,4-methylenedioxy-Ph	2,4,5-triOCH_3-Ph	**10**	3,4-methylenedioxy-Ph	2,4,6-triOCH_3-Ph
11	3,4-methylenedioxy-Ph	3,4,5-triOCH_3-Ph	**12**	3,4-methylenedioxy-Ph	3,4-methylenedioxy-Ph
13	3,4-methylenedioxy-Ph	4-CH_3-Ph	**14**	3,4-methylenedioxy-Ph	4-$N(CH_3)_2$-Ph
15*	3,4-methylenedioxy-Ph	2-naphthyl	**16**	3,4-methylenedioxy-Ph	1-naphthyl
17*	3,4-methylenedioxy-Ph	2,6-diOCH_3-Ph	**18**	3,4-methylenedioxy-Ph	4-$O(CH_2)_3CH_3$-Ph
19	3,4-methylenedioxy-Ph	4-F-Ph	**20***	3,4-methylenedioxy-Ph	2-F-Ph
21	3,4-methylenedioxy-Ph	Ph	**22***	3,4-methylenedioxy-Ph	2-NO_2-Ph
23	3,4-methylenedioxy-Ph	2-Cl-Ph	**24**	3,4-methylenedioxy-Ph	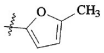
25	3,4-methylenedioxy-Ph	3-OCH_3-Ph	**26**	3,4-methylenedioxy-Ph	3-OCH_3,4-OH-Ph
27	3,4-methylenedioxy-Ph		**28**	3,4-methylenedioxy-Ph	3-OCH_3,4-Obenzyl-Ph
29	3,4-methylenedioxy-Ph	2,5-diOCH_3-Ph	**30**	3,4-methylenedioxy-Ph	3,4-diOCH_3-Ph
31*	3,4-methylenedioxy-Ph	4-CN-Ph	**32***	3,4-methylenedioxy-Ph	3-CF_3,4-Cl-Ph
33*	3,4-methylenedioxy-Ph	4-CF_3-Ph	**34***	3,4-methylenedioxy-Ph	3-CF_3-Ph
35*	3,4-methylenedioxy-Ph	3,5-Cl_2-Ph	**36***	3,4-methylenedioxy-Ph	2,4-Cl_2-Ph
37*	3,4-methylenedioxy-Ph	3-Br-Ph	**38***	3,4-methylenedioxy-Ph	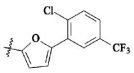
39*	3,4-methylenedioxy-Ph	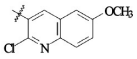	**40***	3,4-methylenedioxy-Ph	
41*	3,4-methylenedioxy-Ph	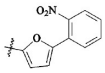	**42***	3,4-methylenedioxy-Ph	2,3,4-triOCH_3-Ph
43	4-NO_2-Ph	3,4-methylenedioxy-Ph	**44**	3-NO_2-Ph	3,4-methylenedioxy-Ph
45	2,4-diOCH_3-Ph	3,4-methylenedioxy-Ph	**46**	2,4,5-triOCH_3-Ph	3,4-methylenedioxy-Ph
47	2,4,6-triOCH_3-Ph	3,4-methylenedioxy-Ph			

[a](a) KOH 50% w/v, methanol, rt, 24 h. *Novel compounds. Ph = phenyl.

regulator of membrane fusion, as a MtbPtpA substrate. PtpA enters into host macrophages and dephosphorylates the cytoplasmic protein VPS33B, inhibiting the maturation of phagosomes, and therefore, preventing their fusion with lysosomes, a mechanism by which macrophages promote their microbicidal activity.[12] Hence, PtpA was recognized as the first enzyme of Mtb that interacts directly with an identified substrate of the host. Due to the fact that PTPs of Mtb modulate phosphorylated proteins of the host, it was believed that Mtb lacked tyrosine kinases proteins.[4] However, it was recently identified in Mtb a protein tyrosine kinase (PtkA), which has PtpA as substrate, although PtkA is not a substrate for PtpA.[13]

Regarding MtbPtpB, its genetic inactivation accelerated mycobacterial cell death in interferon-γ (IFN-γ) activated macrophages and severely reduced the bacterial load in guinea pigs.[14] Recently, Zhou and co-workers hypothesized that MtbPtpB could promote mycobacterial survival in the host by targeting the IFN-γ mediated signaling pathway.[15] These findings elegantly demonstrate that MtbPtpB subverts the innate immune responses by blocking extracellular signal-regulated kinases 1 and 2 (ERK1/2) and p-38 mediated by IFN-γ stimulated interleukin 6 (IL-6) production and promotes host cell survival by activating the Akt pathway and blocking caspase-3 activity.[15] Moreover, Bach and co-workers[12] and Zhou and co-workers[15] demonstrated that PtpA and PtpB are essential for intracellular bacterial persistence, suggesting that the inactivation of these enzymes reduces the growth of Mtb in human macrophages. Because of the significant regulatory role in the cell signaling, dysfunctions of activity in the human PTPs provoke diseases such as cancer, diabetes, neurologic, and autoimmune disorders. For these reasons, PTPs appear as important therapeutic targets.[16−18] In line with this, the specific inhibition of MtbPtpA and MtbPtpB emerges as a highly promising new approach for TB therapy.[15,18,19]

Scheme 2. Synthesis of Chalcone Derivatives 48−100[a]

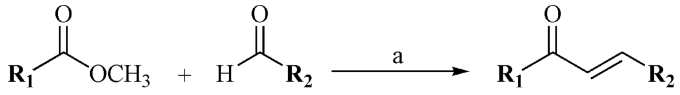

48-100

Comp.	R_1	R_2	Comp.	R_1	R_2
48	2-naphthyl	3-NO_2-Ph	**49**	2-naphthyl	4-NO_2-Ph
50	2-naphthyl	2-NO_2-Ph	**51**	2-naphthyl	4-Cl-Ph
52*	2-naphthyl	3,4-Cl_2-Ph	**53**	2-naphthyl	2,6-Cl_2-Ph
54	2-naphthyl	3-Cl-Ph	**55**	2-naphthyl	2-Cl-Ph
56	2-naphthyl	Ph	**57**	2-naphthyl	4-CH_3-Ph
58	2-naphthyl	4-OCH_3-Ph	**59**	2-naphthyl	3-OCH_3-Ph
60	2-naphthyl	2,6-diOCH_3-Ph	**61**	2-naphthyl	2,4,5-triOCH_3-Ph
62*	2-naphthyl	4-$O(CH_2)_3CH_3$-Ph	**63**	2-naphthyl	4-F-Ph
64*	2-naphthyl	2-F-Ph	**65**	2-naphthyl	4-Br-Ph
66	2-naphthyl	3,4-methylenedioxy-Ph	**67**	2-naphthyl	2-naphthyl
68	2-naphthyl	1-naphthyl	**69**	2-naphthyl	
70	2-naphthyl	4-COOH-Ph	**71**	2-naphthyl	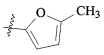
72*	2-naphthyl	2,5-diOCH_3-Ph	**73***	2-naphthyl	2,4,6-triOCH_3-Ph
74*	2-naphthyl	3-OCH_3,4-Obenzyl-Ph	**75***	2-naphthyl	3,5-Cl_2-Ph
76*	2-naphthyl	3-CF_3-Ph	**77***	2-naphthyl	4-CF_3-Ph
78*	2-naphthyl	3-CF_3,4-Cl-Ph	**79**	2-naphthyl	4-CN-Ph
80	2-naphthyl	3-Br-Ph	**81**	2-naphthyl	2,4-Cl_2-Ph
82*	2-naphthyl	2,3,4-triOCH_3-Ph	**83***	2-naphthyl	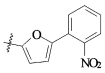
84*	2-naphthyl	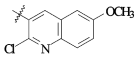	**85**	4-Br-Ph	2-naphthyl
86*	2,4,5-triOCH_3-Ph	2-naphthyl	**87**	3,5-diOCH_3-Ph	2-naphthyl
88*	2,5-Cl_2-Ph	2-naphthyl	**89***	3,4-Cl_2-Ph	2-naphthyl
90*	3-OCH_3-Ph	2-naphthyl	**91***		2-naphthyl
92*		2-naphthyl	**93***		2-naphthyl
94	4-CH_3–Ph	2-naphthyl	**95***		2-naphthyl
96*	2,4-diOCH_3-Ph	3-OCH_3,4-Obenzyl-Ph	**97***	4-Br-Ph	3-OCH_3,4-Obenzyl-Ph
98*	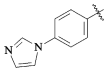	3-OCH_3,4-Obenzyl-Ph	**99***		3-OCH_3,4-Obenzyl-Ph
100*	2,5-diOCH_3-Ph	3-OCH_3,4-Obenzyl-Ph			

[a](a) KOH 50% w/v, methanol, rt, 24 h. *Novel compounds. Ph = phenyl.

The pioneers in the description of MtbPtpA inhibitors, Waldmann and co-workers, have tested analogues of the natural products stevastelin, roseofilin, and prodigiosins, obtaining IC_{50} values ranging from 8.8 to 28.7 μM.[20] Later, sodium molybdate, orthovanadate, and tungstate were characterized as reversible inhibitors of PtpA.[21] Ellman and co-workers also identified a benzanilide derivative as selective inhibitor of PtpA, with a K_i value of 1.4 μM.[22]

In the search for MtbPtpB inhibitors, Alber and co-workers studied the sulfonamide derivative (oxalylamino-methylene)-thiophene sulfonamide (OMTS), which showed high specificity and selectivity for this protein in comparison with other human PTPs, with an IC_{50} value of 0.44 μM.[23] They also identified a series of indole derivatives as PtpB inhibitors, showing selectivity indexes up to about 100.[24] Isoxazoles were found as competitive inhibitors of PtpB, with the most selective inhibitor presenting high affinity with a K_i value of 0.22 μM.[25] More recently, thiazolidinones spiro-fused to indolinones and sulfonylhidrazones were also identified as MtbPtpB inhibitors.[26]

In recent years, we have described the inhibitory potency of a series of naphthylchalcones against MtbPtpA, with the most potent compound exhibiting an IC_{50} value of 8.4 μM.[27] These are competitive and selective inhibitors of MtbPtpA, which additionally showed significant growth inhibitory activity of Mtb in infected macrophages.[28] Yoon and co-workers also identified licochalcone A derivatives as inhibitors of PTPs (human PTP1B).[29] Similarly, many classes of compounds were assayed in cultures of Mtb,[30] and only three studies were conducted with chalcones;[31−33] nevertheless, no information about the molecular target of these compounds was reported. Therefore, the interest in this class of compounds has grown rapidly not only by its general chemistry and biological properties but also by the need for new anti-TB drugs.

As part of our research program aimed at developing new lead candidates for TB therapy,[27,28] we have selected chalcones,

Table 1. Yields of the Synthesis and Percentage of Inhibition of MtbPtpA and MtbPtpB at a Single Concentration of 25 μM[a]

compd	yield (%)	MtbPtpA inhibition (%)	MtbPtpB inhibition (%)	compd	yield (%)	MtbPtpA inhibition (%)	MtbPtpB inhibition (%)
1	93	38 ± 4	0	**2**	78	23 ± 3	0
3	90	13 ± 2	0	**4**	94	35 ± 5	0
5	98	35 ± 1	10 ± 8	**6**	94	23 ± 2	22 ± 8
7	93	37 ± 7	9 ± 8	**8**	95	17 ± 1	11 ± 2
9	88	19 ± 2	19 ± 5	**10**	78	5 ± 1	0
11	92	5 ± 2	0	**12**	89	6 ± 4	0
13	78	14 ± 1	0	**14**	53	10 ± 1	0
15	91	12 ± 2	15 ± 2	**16**	91	8 ± 2	0
17	87	4 ± 2	0	**18**	93	11 ± 4	0
19	87	0	0	**20**	93	9 ± 3	0
21	61	0	0	**22**	15	0	43 ± 4
23	88	5 ± 3	0	**24**	87	40 ± 6	8 ± 6
25	93	10 ± 2	0	**26**	44	0	0
27	92	7 ± 1	0	**28**	88	12 ± 4	0
29	96	10 ± 1	0	**30**	41	19 ± 2	0
31	97	4 ± 2	0	**32**	85	0	0
33	96	7 ± 1	0	**34**	87	41 ± 10	0
35	92	14 ± 3	0	**36**	84	27 ± 9	0
37	97	5 ± 2	0	**38**	93	36 ± 6	16 ± 6
39	95	29 ± 5	0	**40**	62	19 ± 6	0
41	99	19 ± 5	10 ± 3	**42**	94	26 ± 1	9 ± 4
43	82	33 ± 1	34 ± 2	**44**	40	26 ± 12	6 ± 3
45	95	42 ± 5	0	**46**	90	8 ± 4	29 ± 12
47	78	0	15 ± 3	**48**	97	12 ± 1	7 ± 2
49	96	18 ± 2	39 ± 7	**50**	20	10 ± 1	32 ± 8
51	74	13 ± 2	27 ± 3	**52**	96	11 ± 2	28 ± 5
53	75	16 ± 3	0	**54**	93	7 ± 1	0
55	29	0	13 ± 4	**56**	88	4 ± 1	16 ± 2
57	89	8 ± 2	28 ± 6	**58**	89	35 ± 7	0
59	79	10 ± 2	0	**60**	94	40 ± 1	24 ± 10
61	67	7 ± 1	0	**62**	95	8 ± 3	17 ± 4
63	99	13 ± 3	14 ± 5	**64**	92	23 ± 1	0
65	82	8 ± 3	24 ± 4	**66**	91	13 ± 2	0
67	93	39 ± 3	25 ± 3	**68**	96	43 ± 11	0
69	66	15 ± 5	0	**70**	97	9 ± 1	70 ± 3
71	92	30 ± 2	0	**72**	99	22 ± 4	0
73	93	49 ± 4	0	**74**	63	5 ± 2	0
75	94	19 ± 2	29 ± 3	**76**	91	24 ± 4	0
77	93	43 ± 16	37 ± 6	**78**	44	13 ± 6	0
79	95	21 ± 3	20 ± 5	**80**	90	0	20 ± 12
81	98	10 ± 1	47 ± 19	**82**	81	0	0
83	86	9 ± 1	7 ± 4	**84**	99	22 ± 3	17 ± 7
85	88	11 ± 6	42 ± 5	**86**	72	22 ± 4	14 ± 5
87	89	0	10 ± 4	**88**	96	0	20 ± 6
89	97	9 ± 2	18 ± 2	**90**	98	0	0
91	88	40 ± 2	0	**92**	70	0	24 ± 8
93	10	16 ± 1	37 ± 6	**94**	82	10 ± 4	34 ± 10
95	97	31 ± 4	49 ± 6	**96**	18	40 ± 7	0
97	87	63 ± 12	0	**98**	90	38 ± 3	0
99	55	5 ± 1	19 ± 8	**100**	91	12 ± 1	16 ± 2

[a]The results are shown as the average percentage of the individual mean (± SD, standard deviation) for three experiments.

which are intermediates in flavonoid biosynthesis in plants, as a new promising scaffold for MtbPtps inhibition. In this work, we have synthesized and evaluated a library of 100 chalcone against both MtbPtpA and MtbPtpB. The results achieved led to the determination of potency and investigation of the structure–activity relationships (SAR), mechanism of inhibition, selectivity, and mode of interaction of this series. The integration of design, synthesis, biological evaluation, molecular modeling, and SAR studies has proven useful for the identification of a new series of competitive and selective inhibitors of MtbPtpA and MtbPtpB.

2. RESULTS AND DISCUSSION

2.1. Chemistry. A chemical library of 100 chalcone derivatives was prepared by aldolic condensation of aromatic aldehydes and corresponding acetophenones (Schemes 1 and

2), with yields ranging from 10 to 99% (Table 1). Compounds **1−42** are derived from 3,4-methylenedioxyacetophenone; compounds **43−47** are derived from 3,4-methylenedioxybenzaldehyde; compounds **48−84** are derived from 2-naphthylacetophenone; compounds **85−95** are derived from 2-naphthaldehyde, while compounds **96−100** are derived from benzylated vanillin. All reagents used were commercially available, except benzylated vanillin (3-methoxy-4-(phenylmethoxy)-benzaldehyde) (prepared as previously described, with yield of 88%),[34] 2,4,5-trimethoxyacetophenone (synthesized as previously described with yield of 81%),[35] and 2,4,6-trimethoxyacetophenone (synthesized as previously described with yield of 85%).[36]

Compounds **43−47** and **85−95** were designed to complement the chalcone series previously assayed against MtbPtpA[27] and compounds **96−100** to promote variations in the B-ring, maintaining promising substituents on the ring A. The strategy used for the synthesis of the other chalcones (**1−42** and **48−84**) was the inversion of the rings of that previously published series.[27] Because all the compounds have at least one aromatic ring, we selected the substituents first based on the Manual Method of Topliss,[37a] which comprises a fixed group of susbtituents to the aromatic mono- or disubstituted ring. Moreover, we expanded the series by the inclusion of other substituents and rings, promoting greater structural diversity. Still, it is noteworthy that all compounds were designed and fit in the "rule of five" (or Lipinski Rule).[37b]

All synthesized compounds, including those previously reported by other authors (chalcones derivatives **1**, **5−14**, **19**, **21**, **25**, **26**, **28−30**, **43**, **45**, **46**, **50**, **70**, **79−81**, **87**, and **94**)[38] or by us (**3**, **16**, **18**, **23**, **24**, **27**, **44**, **47−49**, **51**, **53−61**, **63**, **65−69**, **71**, and **85**)[36b,39] were characterized by ^{1}H NMR, ^{13}C NMR, and IR (Supporting Information). The spectral characterization (^{1}H NMR, ^{13}C NMR, IR, and elementary analysis) of the novel compounds (**2**, **4**, **15**, **17**, **20**, **22**, **31−42**, **52**, **62**, **64**, **72−78**, **82−84**, **86**, **88−93**, and **95−100**) is detailed in the Experimental Section of the Supporting Information. ^{1}H NMR spectra revealed that all structures are configured *E* ($J_{H\alpha-H\beta}$ = ∼16 Hz).

2.2. Biochemical Evaluation and SAR Studies. The inhibitory activity of the chalcone derivatives against MtbPtpA and MtbPtpB was evaluated according to the standard method described elsewhere.[27] The percentage of inhibition was assessed at a single concentration of 25 μM for each compound of the series (Table 1). As can be seen, several chalcone derivatives were active against both enzymes. In the case of MtbPtpA, the percentage of inhibition varied from 0 to 63%. Specifically, the results indicate that 25 out of 100 compounds (**1**, **4**, **5**, **7**, **24**, **34**, **36**, **38**, **39**, **42−45**, **58**, **60**, **67**, **68**, **71**, **73**, **77**, **91**, and **95−98**) exhibited enzyme inhibition (inhibition >25%). Regarding the MtbPtpB enzyme, 11 out of 100 compounds (**22**, **43**, **49**, **50**, **70**, **77**, **81**, **85**, and **93−95**) showed inhibition >30%.

To better understand the molecular aspects involved in the inhibition of mycobacterium PTPs enzymes, we have determined IC_{50} values for all compounds presenting inhibitions higher than 25% and 30% for MtbPtpA and MtbPtpB, respectively (Table 2). The results indicate that compounds **5**, **7**, **39**, **42−44**, **58**, **67**, **68**, **95**, and **96** showed substantial inhibition of MtbPtpA with IC_{50} values <100 μM (Table 2). Compounds **1**, **4**, **24**, **34**, **38**, **45**, **91**, and **98** were moderate inhibitors (IC_{50s} from 100 to 200 μM), while compounds **36**, **60**, **71**, **73**, **77**, and **97** showed modest inhibition of MtbPtpA (IC_{50s} > 200 μM). The best inhibitory effect of MtbPtpA was achieved by compound **96** (IC_{50} = 15 μM), derived from benzylated vanillin structure, with methoxyl groups at positions 2 and 4 at the A-ring. In general, the 2-naphthyl group as B-ring (compound **95**) seems to favorably contribute to MtbPtpA inhibition. This observation is in good agreement with previous data that indicated significant $\pi-\pi$ interactions between the 2-naphthyl substituent and the side-chain of the Trp48 amino acid residue of the MtbPtpA binding site.[27,28] On the basis of the molecular information collected in the course of this work, the hydrophobicity of the B-ring as well as the presence of hydrogen bond donor/acceptor substituents in the A-ring seem to play an important role in the inhibitory activity of this series. Similar results were obtained for a series of chalcone-like derivatives evaluated against H37Rv Mtb strain.[31] In that work, the most active compounds presented hydrophobic B-rings and polar-substituted A-rings.

Table 2. IC_{50} Values for a Series of MtbPtpA and MtbPtpB Inhibitors[a]

compd	MtbPtpA IC_{50} (μM)	MtbPtpB IC_{50} (μM)	compd	MtbPtpA IC_{50} (μM)	MtbPtpB IC_{50} (μM)
1	117 ± 17	nd	**4**	151 ± 7	nd
5	74 ± 7	nd	**7**	66 ± 26	nd
22	nd	81 ± 4	**24**	169 ± 15	nd
34	155 ± 7	nd	**36**	407 ± 18	nd
38	174 ± 36	nd	**39**	93 ± 4	nd
42	83 ± 17	nd	**43**	62 ± 9	**51 ± 8**
44	**45 ± 6**	nd	**45**	101 ± 20	nd
49	nd	62 ± 8	**50**	nd	54 ± 5
58	93 ± 11	nd	**60**	214 ± 22	nd
67	93 ± 6	nd	**68**	93 ± 10	nd
70	nd	**12 ± 2**	**71**	1023 ± 12	nd
73	1659 ± 37	nd	**77**	331 ± 28	339 ± 18
81	nd	417 ± 60	**85**	nd	**25 ± 6**
91	100 ± 5	nd	**93**	nd	81 ± 6
94	nd	135 ± 9	**95**	**32 ± 4**	57 ± 4
96	**15 ± 4**	nd	**97**	302 ± 24	nd
98	102 ± 12	nd			

[a]The results are shown as the average of the individual mean (± SD) for 3 experiments. SD = standard deviation; nd = not determined.

In the case of MtbPtpB, eight compounds (**22**, **43**, **49**, **50**, **70**, **85**, **93**, and **95**) exhibited significant inhibition with IC_{50} values <100 μM (Table 2). Compound **94** (IC_{50} ∼ 135 μM) showed moderate inhibition, while compounds **77** (IC_{50} ∼ 339 μM) and **81** (IC_{50} ∼ 417 μM) exhibited low inhibitory potency. The most potent inhibitor of this series, compound **70** (IC_{50} = 12 μM), bears the 2-naphthyl and the 4-carboxy-phenyl groups as A- and B-ring, respectively. The crystallographic binding mode of the potent inhibitor of MtbPtpB, OMTS, indicated that the carboxylic acid substituent is important for ligand binding and affinity.[23] The 2-naphthyl substituent is also likely to play a major role in the inhibition of MtbPtpB, regardless of whether it is A- or B-ring (e.g., compounds **50**, **85**, and **95**; IC_{50} = 54, 25, and 57 μM, respectively). The presence of bulky (compound **85**) or electron withdrawing (compounds **49**, **50**, and **70**) substituents in the phenyl group (B-ring) is favorable for the inhibitory potency. In addition, the bioisosteric replacement of the phenyl moiety with a pyrrole (compound **93**) or 3-chlorotiophene (compound **95**) is well tolerated.

2.3. Selectivity Assay. In general, SAR investigations focus on the biological activity against single targets (e.g., potency,

affinity). Nevertheless, it is well-known that a number of compounds bind to different targets (e.g., homologous enzymes) in different ways, revealing the importance of the selectivity in drug design.[40] In this direction, the three most potent inhibitors of MtbPtpA and MtbPtpB (compounds **43**, **44**, **70**, **85**, **95**, and **96**) were further evaluated against the human tyrosine phosphatase PTP1B (Table 3). The selectivity indexes obtained indicated that structural features play a key role on selectivity of this class of inhibitors. For example, compounds **44** and **95** exhibited moderate selectivity toward MtbPtpA (2.4- and 3.1-fold, respectively). In contrast, compound **96**, which bears a 4-benzyloxy substituent in the B-ring, was highly selective toward MtbPtpA (about 18-fold). Regarding the MtbPtpB inhibitors, compound **43** showed a moderate shift toward the opposite way, being selective for the human enzyme, while compound **85** showed no selectivity. Conversely, compound **70**, having a benzoic acid as B-ring, exhibited not only improved potency (IC_{50} = 12 μM) but also extraordinary 258-fold selectivity for MtbPtpB. With the goal of shedding light on the mechanism of inhibition of this series, these compounds were selected for further kinetic studies.

Table 3. Values of IC_{50} and Selectivity Indexes for a Small Series of Inhibitors against MtbPtpA, MtbPtpB, and Human PTP1B[a]

compd	MtbPtpA IC_{50} (μM)	MtbPtpB IC_{50} (μM)	PTP1B IC_{50} (μM)	SI
43	>100	51 ± 8	23 ± 2	0.5**
44	45 ± 6	>100	107 ± 2	2.4*
70	>100	12 ± 2	3090 ± 168	258**
85	>50	25 ± 6	29 ± 2	1.2**
95	32 ± 4	>50	100 ± 5	3.1*
96	15 ± 4	>100	263 ± 3	18*

[a]The results are shown as the average of the individual mean ± SD. SI = selectivity index, given by *($IC_{50}^{PTP1B}/IC_{50}^{MtbPtpA}$) or **($IC_{50}^{PTP1B}/IC_{50}^{MtbPtpB}$).

2.4. Kinetics Measurements and Mechanism of Inhibition. The definition of the mode of inhibition and binding relationships between the free enzyme (E), substrate (S), and enzyme−substrate (E•S) species to the inhibitor (I) allows the development of mechanism-based SARs, which are highly desirable for the rational design of enzyme inhibitors.[41] To this end, we have determined the type of inhibition with respect to the substrate *p*-nitrophenyl phosphate (pNPP). Overall, the inhibitors exhibited degrees of saturation and release of *p*-nitrophenol that follows a classic Michaelis−Menten enzymatic mechanism.[42] The Lineweaver−Burk double-reciprocal plots show intercepts of all lines (obtained at least with three different inhibitor concentrations) converging at the *y*-axis ($1/V_{max}$), whereas the slope (K_{mapp}/V_{max}) and *x*-axis intercepts ($-1/K_{mapp}$) vary with inhibitor concentration (Figure 1). In these assays, the V_{max} remains constant and the K_{mapp} values increase with increasing inhibitor concentrations. The behavior is consistent with a mutually exclusive binding mode, where the inhibitors compete with the substrate for the binding to the free enzyme active site.[43] Therefore, the evaluated compounds are competitive inhibitors of MtbPtpA (compounds **44**, **95**, and **96**) and MtbPtpB (compounds **43**, **70**, and **85**). The K_i values obtained are in the low micromolar range (12−29 μM for MtbPtpA, and 8−13 μM for MtbPtpB) (Table 4), indicating that these inhibitors, containing a new chemical scaffold for PtpB inhibition, are attractive lead compounds for further optimization.[27,28]

2.5. Molecular Modeling. The integration of experimental and computational methods is an extremely attractive strategy for the design and optimization of anti-infective lead candidates.[44] On the basis of the information obtained from the enzymatic assays, molecular modeling studies were performed as a crucial step toward understanding the mode of interaction of these potent and selective inhibitors. To achieve this, the high affinity inhibitors **96** (K_i = 12 μM) and **70** (K_i = 8 μM) were docked into the active site of MtbPtpA and MtbPtpB, respectively (Figure 2). Although a quantitative agreement between model and experimental SAR data was not expected, the models provided relevant insights into the molecular aspects underlying the inhibitory activity of the chalcone derivatives.

For instance, the predicted binding mode of compound **96** (K_i = 12 μM) within the MtbPtpA binding site indicates that the inhibitor adopts an extended conformation (Figure 2A). In this conformation, polar interactions play a key role in orientating the inhibitor within the binding site, specifically, the carbonyl group and the 2-methoxyphenyl substituent of the A-ring showed a bidentate hydrogen bond interaction with the conserved Arg17 residue, while the oxygen atom of the 4-benzyloxy substituent is in a favorable position to accept a hydrogen bond from the side-chain of His49. Simultaneously, the electronegative oxygen atom of the 3-methoxy substituent in the B-ring is complementary to the helix dipole of helix α1. In addition, favorable nonpolar interactions assist the stabilization of the inhibitor. According to the model, three $\pi-\pi$ interactions considerably contribute to the inhibitory potency: (i) between the 2,4-dimethoxyphenyl substituent (A-ring) and the side-chain of Asn92, (ii) between the central phenyl ring (B-ring) and the side-chain of the catalytic Asp126, and (iii) between the aromatic ring of the 4-benzyloxy substituent and the side-chain of Tyr128, which adopts a classic parallel-displaced arrangement.

Despite the overall similarities in the active site, the comparison between mycobacterium and human PTPs revealed significant structural differences. The analysis indicated that MtbPtpA has a crevice formed by the Trp48, Tyr128, and Tyr129 side-chains, which generates an additional hydrophobic pocket within the binding site of the mycobacterium enzyme.[5] Furthermore, the electrostatic potential in the MtbPtpA active site cavity is notably different compared with the human homologue. The presence of the His49 and Ser52 residues in MtbPtpA (Glu50 and Asn53 in human HCPTPA) suggests a change in pattern of charge distribution around the wall of the crevice (Figure 3A). The binding mode of **96** explores the structural differences between human and mycobacterium enzymes. The model shows that the benzyl group of the 4-benzyloxy substituent is sandwiched between the side-chains of Tyr128 and His49, while the oxygen atom of the substituent interacts with the side-chain NE2 of His49.

The proposed binding mode of compound **70** (K_i = 8 μM) into the MtbPtpB active site indicates that the competitive inhibitor occupies the narrow channel close to the catalytic Cys160 (Figure 2B). In this conformation, the inhibitor establishes attractive polar and hydrophobic contacts with the MtbPtpB active site residues. The negatively charged carboxyl group of compound **70** is attracted by the positively charged side-chain of Arg210 and the electronegative carbonyl substituent is complementary to the helix dipole of helix α5,

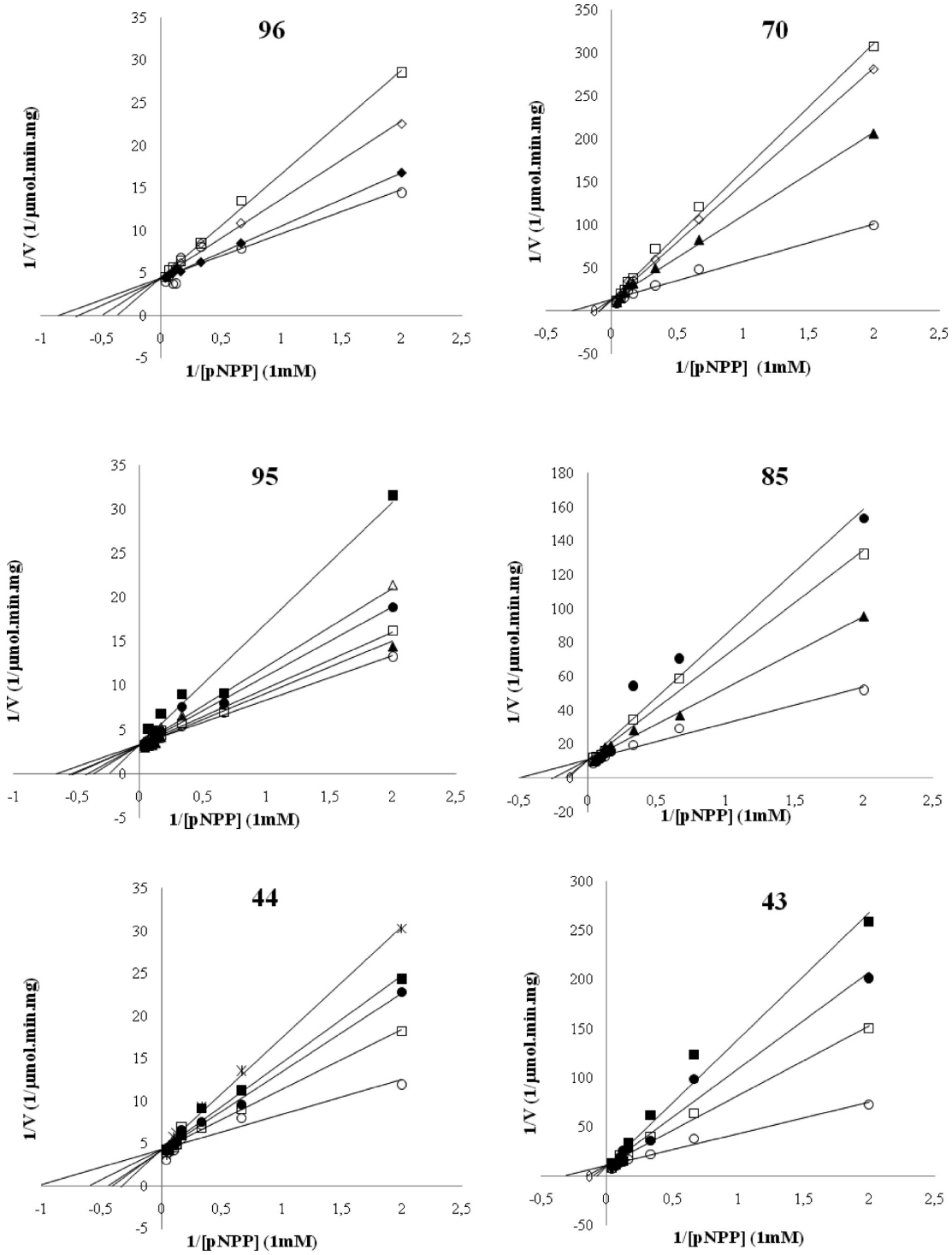

Figure 1. Competitive inhibitory profile of compounds **96**, **95**, and **44** against MtbPtpA, and of compounds **70**, **85**, and **43** against MtbPtpB. Kinetic experiments were conducted in the presence of increasing concentrations of inhibitors: 0 μM (○), 5 μM (◆), 10 μM (▲), 15 μM (◇), 20 μM (□), 30 μM (●), 40 μM (△), 50 μM (■), 60 μM (×); pNPP was used as substrate in all experiments.

while the electron-rich 2-naphthyl group (B-ring) undergoes π-stacking with the side-chain of the Arg166. Additionally, the nonpolar parts of compound **70** make favorable van der Waals contacts with several structural elements of the protein, some of them establishing hydrophobic interactions with the macromolecular counterparts, which significantly contribute to the complex stability. In particular, the aromatic ring of the benzoic acid substituent (A-ring) is in van der Waals contacts to the side-chain of Met206 and the 2-naphthyl group (B-ring) is docked into the hydrophobic pocket formed by the amino acid residues Phe80, Pro81, and Phe133.

The predicted interaction mode of compound **70** within the MtbPtpB binding site not only indicated the structural elements that might be related to the binding affinity but also provided insights into the molecular basis for selectivity. The protein tyrosine phosphatase family shares a catalytic domain

Table 4. K_i Values of the MtbPtpA and MtbPtpB Inhibitors[a]

compd	MtbPtpA K_i (μM)	MtbPtpB K_i(μM)	IC_{50}/K_i
43		13 ± 1	3.8
44	29 ± 1		1.5
70		8 ± 1	1.4
85		10 ± 1	2.6
95	23 ± 1		1.4
96	12 ± 1		1.3

[a] K_i values are shown as the average of the individual mean ± SD.

containing a four-stranded parallel β-sheets that connects to a helix (helix α5) through a loop known as *P loop*. The *P loop* (residues 160−166) harbors the catalytic Cys160 within the invariant sequence HCX_5R (Figure 3B).[7] According to the proposed binding mode, the inhibitor is in favorable orientation to form van der Waals interactions with the side-chain of Phe161 (Figure 2B). The hydrophobic Phe161 residue is replaced with a polar Ser216 residue in the human homologue (Figure 3B). Therefore, the nonconservative substitution considerably changes the molecular recognition features of the binding sites. This finding is in good agreement with the experimental kinetic evaluation and might explain the high selectivity of the inhibitor **70** (∼260-fold) toward the mycobacterium enzyme (Table 3).

3. CONCLUSIONS

Our approach exploring the design, synthesis, and biological evaluation led to identification of a small series of chalcone derivatives as competitive inhibitors of MtbPtpA (**44**, **95**, and **96**) and MtbPtpB (**43**, **70**, and **85**). The predicted binding mode for the selective MtbPtpA inhibitor **96** shows polar interactions that play a key role in the orientation of this compound within the protein binding site as well as favorable nonpolar interactions that assist the stabilization of the inhibitor in the cavity. For the highly selective MtbPtB inhibitor **70**, the proposed binding mode indicates that this compound occupies the narrow channel close to the catalytic Cys160, establishing attractive polar and hydrophobic contacts with the MtbPtpB active site residues. Their chemical versatility, activity, and selectivity suggest this class of competitive inhibitors as promising lead compounds for further medicinal chemistry efforts for the development of new anti-TB drugs.

4. MATERIALS AND METHODS

4.1. Preparation of Compounds. Reagents used were obtained commercially (Sigma-Aldrich), except benzylated vanillin (3-methoxy-4-(phenylmethoxy)-benzaldehyde), 2,4,5-trimethoxyacetophenone, and 2,4,6-trimethoxyacetophenone, which were synthesized as previously described.[34−36]

Chalcone derivatives (**1**−**25** and **27**−**100**) were prepared by aldolic condensation between acetophenones (1.0 mmol) and corresponding aldehydes (1.0 mmol), in methanol (15 mL), KOH (50% w/v), at room temperature with magnetic agitation for 24 h; the volume of KOH varied according to the reaction. When the aldehyde had photosensitive groups, the reactions were made in absence of light. Distilled water and 10% hydrochloric acid were added to the reaction for total precipitation of the compounds, which were then obtained by vacuum filtration and later recrystallized in dichloromethane and hexane. The purity of the synthesized compounds was analyzed by thin-layer chromatography (TLC) using Merck silica precoated aluminum plates of 200 μm thickness, with several solvent systems of different polarities. Compounds were visualized with ultraviolet light (λ = 254 and 360 nm) and using sulfuric anisaldehyde solution followed by heat application as the developing agent.

Compound **26** was obtained by condensation between 3,4-methylenedioxyacetophenone (1.0 mmol) and 3-methoxy-4-hydroxy-

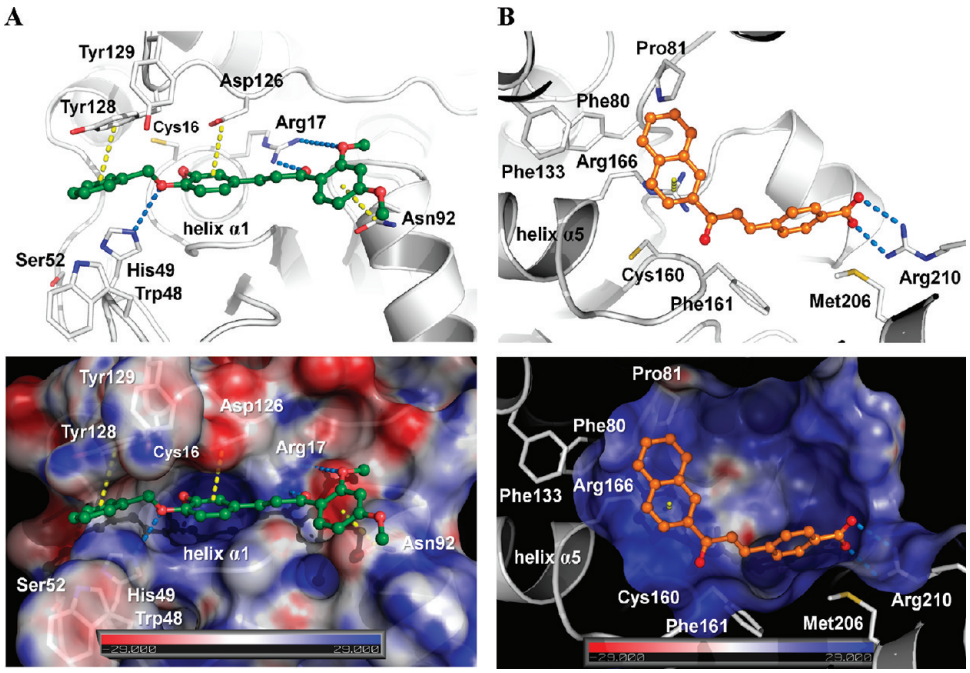

Figure 2. (A) Predicted binding mode of compound **96** within the MtbPtpA active site. (B) Predicted binding mode of compound **70** within the MtbPtpB active site. Upper panel: inhibitors and protein residues involved in the ligand−receptor binding are indicated as ball-and-stick and stick models, respectively. Hydrogen bonds and π−π interactions are illustrated as blue and yellow dashed lines, respectively. Lower panel: view of the active site showing the surface charge distributions of MtbPtpA and MtPtpB. Positive and negative electrostatic potential (kT/e) are indicated in blue and red, respectively. This depiction was generated using the PyMOL APBS tools.

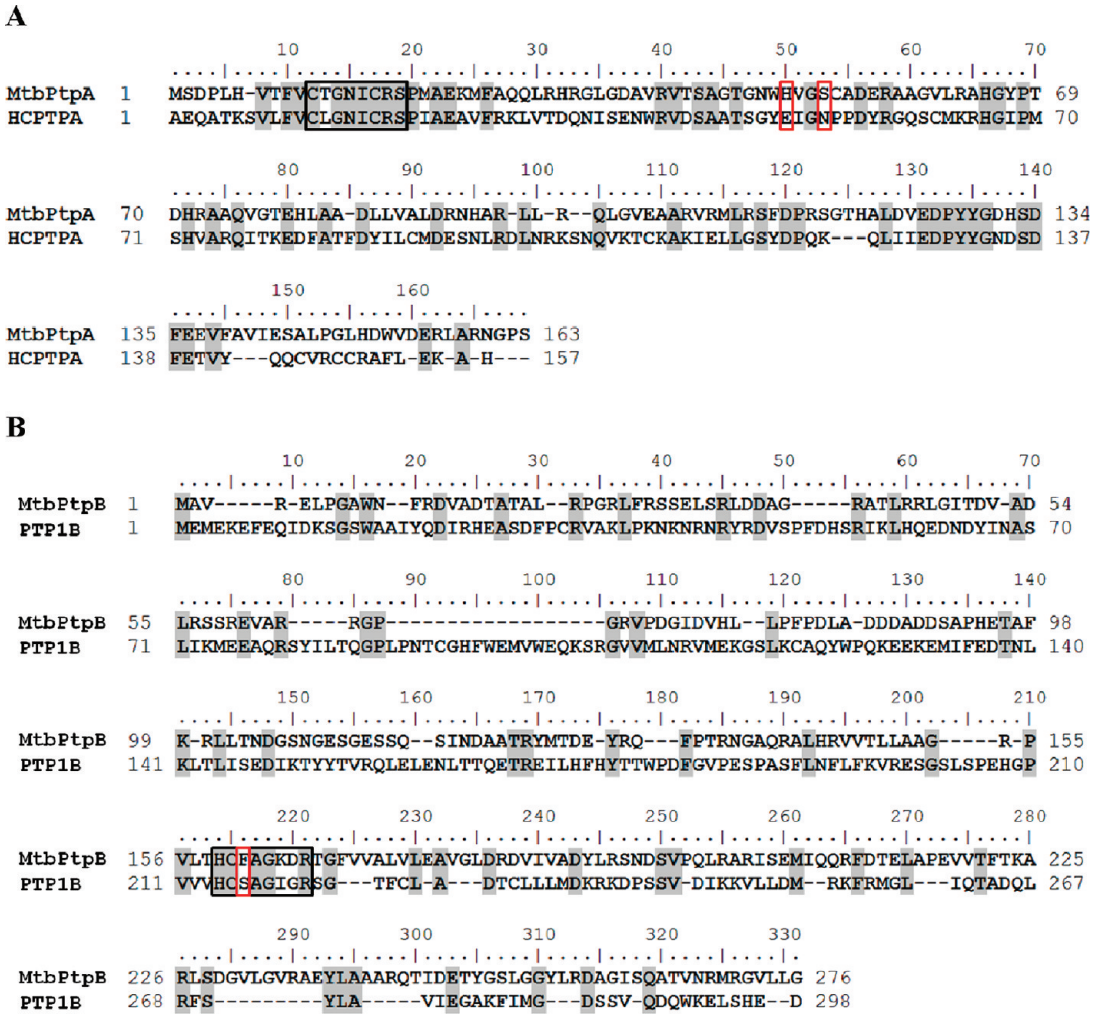

Figure 3. Structure-based sequence alignment of (A) MtbPtpA and HCPTPA and (B) MtbPtpB and PTP1B. Conserved residues are highlighted in gray, and active site signature motifs of the PTP loop are shown in black boxes. The residues presumed to determine inhibitor selectivity that differ from those of human PTPs are shown in red boxes. The pairwise alignment was carried out with BLOSUM62 matrix implemented in BioEdit program.

benzaldehyde (1.0 mmol), in methanol (40 mL), KOH (50% v/v), at reflux for 4 h. Distilled water and 10% hydrochloric acid were added and the solution was left in the freezer for 24 h for total precipitation of the compound, which was obtained by vacuum filtration.

The chalcone derivatives are soluble in dimethylsulfoxide, acetone, acetyl acetate, chloroform, and dichloromethane. Compounds **1**, **5**–**14**, **19**, **21**, **25**, **26**, **28**–**30**, **43**, **45**–**47**, **50**, **70**, **79**–**81**, **87**, and **94** were previously cited in the literature.[38] Chalcones derivatives **3**, **16**, **18**, **23**, **24**, **27**, **44**, **48**, **49**, **51**, **53**–**61**, **63**, **65**–**69**, **71**, and **85** were published by our research group,[36b,39] and **2**, **4**, **15**, **17**, **20**, **22**, **31**–**42**, **52**, **62**, **64**, **72**–**78**, **82**–**84**, **86**, **88**–**93**, and **95**–**100** are novel compounds.

4.2. Physicochemical Data of the Compounds. The structures were confirmed by melting points (mp), infrared spectroscopy (IR), and ^{1}H and ^{13}C nuclear magnetic resonance spectroscopy (NMR), as well as by elementary analysis for the previously undescribed structures. Melting points were determined with a Microquímica MGAPF-301 apparatus and are uncorrected. IR spectra were recorded with an Abb Bomen FTLA 2000 spectrometer on KBr disks. NMR (^{1}H and ^{13}C) spectra were recorded on a Varian Oxford AS-400 (400 MHz) instrument, using tetramethylsilane as an internal standard; ^{1}H NMR spectra revealed that all the structures were geometrically pure and configured *E* ($J_{H\alpha-H\beta}$ = ~16 Hz). Elementary analyses were carried out using a CHNS EA 1110; percentages of C and H were in agreement with the product formula (within ±0.4% of theoretical values for *C*), confirming ≥95% purity. The chemical data for each compound is presented as Supporting Information.

4.3. PTPs Expression and Purification. *(a). PtpA wt and PtpB wt from Mycobacterium tuberculosis.* PtpA and PtpB expression and purification were done as previously described,[45] based in other described methodologies.[46,47]

(b). Human PTP1B wt. The plasmid pET19b encoding the 37 kDa form of the human wild type PTP1B (amino acid residues 1–321) was transformed into *Escherichia coli* BL21(DE3). Expression in *E. coli* BL21(DE3) was under the control of the T7 promoter. *E. coli* cells containing the recombinant plasmid were incubated overnight into 10 mL of LB broth containing 10 μL of ampicillin (100 mM) at 37 °C. Overnigth cultures of *E. coli* BL21(DE3) PTP1B (5 mL) were transferred to 250 mL of LB broth containing 250 μL of ampicillin (100 mM) and were grown with agitation (140 rpm) at 37 °C until an optical density of 0.85 at 600 nm was achieved, induced with IPTG (isopropyl β-D-thiogalactoside) to a final concentration of 0.6 mM. The cultures were grown for additional 20 h at room temperature and were harvested by centrifugation at 8000 rpm for 30 min. The next steps were carried out at 4 °C. The resulting pellet was resuspended in 40 mL of buffer A (20 mM imidazole pH 7.5, 1 mM EDTA, 3 mM DTT, and 10% glycerol) containing protease inhibitors (2 mM benzamidine and 2 μg/mL each of aprotinin, leupeptin, and pepstatin). The cells were lysed by sonication and spun down at 40000 rpm for 30 min. Purification was accomplished by a slight modification of the previously described method.[48] The supernatant

was loaded on a 1 mL HiTrap Q FF column at 1.5 mL/min. The column was washed with buffer A until the absorbance at 280 nm was zero. The protein was eluted at 2 mL/min with a 100 mL linear gradient from zero to 0.5 M NaCl in buffer A. Fractions containing protein were pooled and desalted with a 35 mL HiPrep 26/10 column eluting with buffer B (20 mM bis−tris pH 6.5, 1 mM EDTA, 3 mM DTT, and 10% glycerol). Then, the resulting protein solution was loaded on a 1 mL HiTrap SP FF column at 1.5 mL/min. The column was washed with buffer B until the absorbance at 280 nm was zero. The protein was eluted at 2 mL/min with a 150 mL linear gradient from 0 to 0.5 M NaCl in buffer B. Protein concentrations were monitored by UV ($A_{1\ mg/mL}^{280\ nm}$ = 1.00 mg/mL) and PTP1Bwt yield was 4.5 mg. The PTP1B fractions were stored at −80 °C.

4.4. Measurement of PtpA and PtpB Activity (%) and Inhibition (IC_{50}). The phosphatase assays were carried out as previously described[27] in 96-well plates containing 5 μL of diluted compounds at 1.0×10^{-3} M in DMSO (final concentration of 25 μM), 20 mM imidazol pH 7.0, 40 mM *p*-nitrophenyl phosphate [pNPP], and Milli-Q water to complete 198 μL in each well, followed by addition of 2 μL of recombinant protein in order to start the reaction. The proteins were used in the following concentrations: PtpA 1.0 μg/μL, diluted 5 times in buffer D (20 mM Tris−HCl pH 8.0, 50 mM NaCl, 5 mM EDTA, 20% glycerol, and 5 mM DTT) and PtpB 0.4 μg/μL, diluted 2 times in buffer D; both enzymes in a final concentration of 0.4 μg/μL. The enzymes, when active, cleave the substrate (pNPP), releasing *p*-nitrophenol, which have yellow color. The absorbance was measured by spectrophotometer UV−VIS (TECAN Magellan Infinite M200) for 10 min at 37 °C (at 410 nm with readings every 1 min). Negative controls were performed in the absence of enzyme and compound, and positive controls in the presence of enzyme and 100% DMSO. The percentage of residual activity was calculated as the difference in absorbance between the time 6 and 2 min, obtained by the average of two experiments carried out in triplicate.

The IC_{50} values were determined with increasing concentrations of inhibitor (5−100 μM) versus % of inhibition, in triplicate in two independent experiments. The enzymatic activity was expressed in % of phosphatase residual activity compared with wells without inhibitor. The experimental data were analyzed with SigmaPlot Software 9.0 and the IC_{50} values determined by linear regression. It is important to stress the fact that all compounds are soluble in the assay mixtures at the described experimental conditions.

4.5. Selectivity Assay. The selectivity assays using PTP1B 2.0 μg/μL, diluted 10 times in buffer B (20 mM bis−Tris pH 6.5, 1 mM EDTA, 3 mM DTT, 10% glycerol, and 92 mM NaCl) in a final concentration of 0.2 μg/μL, were carried out as described above.

4.6. Enzyme Kinectics. To determine the mecanism of inhibition, compounds **44**, **95**, and **96** were screened against PtpA and compounds **43**, **70**, and **85** against PtpB, by the same methodology described at section 4.4, however, varying concentrations of pNPP. The K_i values and the mechanism of inhibition of the compounds were determined using increasing concentrations of pNPP (0.5, 1.5, 3, 6, 8, 10, 15, 25 mM) for each concentration of compound (at least three concentrations ranging from 5 to 60 μM). The reaction rates were expressed as specific activity of the protein (μmol pNP min^{-1} mg^{-1}) and the pNPP concentration in mM.

The phosphatase released ($1/V$) was quantified and analyzed by the Lineweaver−Burk plot ($1/[V] \times 1/[S]$) generated in the SigmaPlot Software 9.0. K_{Mapp} values obtained for each compound concentration were plotted versus $[I]$, and the intercept of the curve at *x*-axis corresponding to $-K_i$.

4.7. Molecular Modeling. The 3D structures of the chalcone inhibitors were constructed using standard geometric parameters of the molecular modeling software package SYBYL 8.0. Each single optimized conformation of each molecule in the data set was energetically minimized employing the Tripos force field[49] and the Powell conjugate gradient algorithm[50] with a convergence criterion of 0.05 kcal/mol·Å and Gasteiger−Hückel charges.[51] Molecular docking and scoring protocols were carried out with GOLD 4.1 (Cambridge Crystallographic Data Centre, Cambridge, UK).[52] Default parameters were used to investigate the possible binding conformations of the ligands within the MtbPtpA and MtbPtpB binding pockets. The X-ray crystallographic data for MtbPtpA determined at 1.9 Å (PDB ID 1U2P)[5] and MtbPtpB determined at 2 Å (PDB ID 2OZ5)[7] used in the docking simulations were retrieved from the Protein Data Bank (PDB). The ligands and water molecules from both structures were removed from the binding pockets. Hydrogen atoms were added in standard geometry using the Biopolymer module implemented in SYBYL 8.0. Histidines, glutamines, and asparagines residues within the binding site were manually checked for possible flipped orientation, protonation, and tautomeric states with Pymol 1.2 (DeLano Scientific, San Carlos, USA) side-chain wizard script. The binding site of MtbPtpA was defined as all the amino acid residues encompassed within a 10 Å radius sphere centered on the three-dimensional coordinates of the chloride ion bound to the active site.[5] Similarly, the binding site of MtbPtpB was defined as all the amino acid residues encompassed within a 6 Å radius sphere centered on both the proximal and distal bound inhibitors.[7] The docking procedures were repeated 30 times for each inhibitor. The GOLDScore scoring function and visual inspection were employed to select the representative conformation for each inhibitor.

■ ASSOCIATED CONTENT

Supporting Information

Chemical characterization of the compounds. This material is available free of charge via the Internet at http://pubs.acs.org.

■ AUTHOR INFORMATION

Corresponding Author

*For H.T.: phone, +55 48 3721 6426; fax, +55 48 3721 9672; E-mail, hterenzi@ccb.ufsc.br. For R.J.N.: phone, +55 48 3721 6844 r.236; fax, +55 48 3721 6850; E-mail, nunes@qmc.ufsc.br.

■ ACKNOWLEDGMENTS

We thank Prof. Dr. Pedro M. Alzari (Institut Pasteur, Paris) for the plasmids pRT28a (PtpA and PtpB) and Dr. Tiago A. S. Brandão (Universidade Federal de Minas Gerais) for the plasmid pET19b (PTP1B). We also thank the Departamento de Química—Universidade Federal de Santa Catarina for the equipments for chemical analysis. We thank CNPq, CAPES, FAPESP, MCT, FAPESC, and FINEP for financial support and fellowships.

■ ABBREVIATIONS USED

BCG, Bacillus Calmette-Guérin; DMSO, dimethylsulfoxide; DTT, dithiothreitol; EDTA, ethylenediamine tetraacetic acid; ERK1/2, extracellular signal-regulated kinases 1 and 2; HCPTPA, human cytoplasmic protein tyrosine phosphatase; IFN-γ, interferon-γ; IL-6, interleukin 6; IPTG, isopropyl β-D-thiogalactoside; LMW PTP, low molecular weight protein tyrosine phosphatase; MDR, multidrug-resistance; Mtb, *Mycobacterium tuberculosis*; MtbPtps, *Mycobacterium tuberculosis* protein tyrosine phosphatases; MtbPtpA, *Mycobacterium tuberculosis* protein tyrosine phosphatase A; MtbPtpB, *Mycobacterium tuberculosis* protein tyrosine phosphatase B; OMTS, (oxalylamino-methylene)-thiophene sulfonamide; Ph, phenyl; pNPP, *p*-nitrophenyl phosphate; Ptks, protein tyrosine kinases; PtkA, protein tyrosine kinase A; PTP1B, human protein tyrosine phosphatase 1B; PTPs, protein tyrosine phosphatases; SAR, structure−activity relationships; TB, tuberculosis; TSP PTP, triple specificity protein tyrosine phosphatases; VPS33B, protein sorting 33 homologue B; WHO, World Health Organization

REFERENCES

(1) (a) *Tuberculosis*; available in http://www.who.int/topics/tuberculosis/en/ (accessed January 11, 2011). (b) *Global Tuberculosis Control: Epidemiology, Strategy, Financing: WHO Report 2009*; World Health Organization: Geneva, 2009; 314 pp. Available in http://www.who.int/tb/publications/global_report/2009/pdf/full_report.pdf (accessed January 14, 2011). (c) *TB/HIV Co-infection*; available in http://apps.who.int/tdr/svc/diseases/tb–hiv (accessed January 11 2011).

(2) (a) Ruiz-Manzano, J.; Blanquer, R.; Calpe, J. L.; Caminero, J. A.; Caylá, J.; Domínguez, J. A.; García, J. M.; Vidal, R. Diagnosis and Treatment of Tuberculosis. *Arch. Bronconeumol.* **2008**, *44* (10), 551–566. (b) Ballell, L.; Field, R. A.; Duncan, K.; Young, R. J. New Small-Molecule Synthetic Antimycobacterials. *Antimicrob. Agents Chemother.* **2005**, *49*, 2153–2163. (c) Duncan, K.; Barry, C. E. Prospects for new antitubercular drugs. *Curr. Opin. Microbiol.* **2004**, *7*, 460–465.

(3) Hunter, T. Protein kinases and phosphatases: the yin and yang of protein phosphorylation and signaling. *Cell* **1995**, *80* (2), 225–236.

(4) Cole, S. T.; Brosch, R.; Parkhill, J.; Garnier, T.; Churcher, C.; Harris, D.; Gordon, S. V.; Eiglmeier, K.; Gas, S.; Barry, C. E.; Tekaia, F.; Badcock, K.; Basham, D.; Brown, D.; Chillingworth, T.; Connor, R.; Davies, R.; Devlin, K.; Feltwell, T.; Gentles, S.; Hamlin, N.; Holroyd, S.; Hornsby, T.; Jagels, K.; Krogh, A.; McLean, J.; Moule, S.; Murphy, L.; Oliver, K.; Osborne, J.; Quail, M. A.; Rajandream, M. A.; Rogers, J.; Rutter, S.; Seeger, K.; Skelton, J.; Squares, R.; Squares, S.; Sulston, J. E.; Taylor, K.; Whitehead, S.; Barrell, B. G. Deciphering the biology of *Mycobacterium tuberculosis* from the complete genome sequence. *Nature* **1998**, *393*, 537–544.

(5) Madhurantakam, C.; Rajakumara, E.; Mazumbar, P. A.; Saha, B.; Mitra, D.; Wiker, H. G.; Sankaranarayanan, R.; Das, A. K. Crystal structure of low-molecular-weight protein tyrosine phosphatase from *Mycobacterium tuberculosis* at 1.9-a resolution. *J. Bacteriol.* **2005**, *187*, 2175–2181.

(6) Cowley, S. C.; Babakaiff, R.; Av-Gay, Y. Expression and localization of *Mycobacterium tuberculosis* tyrosine protein phosphatase PtpA. *Res. Microbiol.* **2002**, *153*, 233–241.

(7) Grundner, C.; Ng, H.; Alber, T. *Mycobacterium tuberculosis* Protein Tyrosine Phosphatase PtpB Structure Reveals a Diverged Fold and a Buried Active Site. *Structure* **2005**, *13* (11), 1625–1634.

(8) Beresford, N.; Patel, S.; Armstrong, J.; Szöor, B.; Fordham-Skelton, P.; Tabernero, A.; MptpB, L. A virulence factor from *Mycobacterium tuberculosis*, exhibits triple-specificity phosphatase activity. *Biochem. J.* **2007**, *406*, 13–18.

(9) Koul, A.; Choidas, A.; Treder, M.; Tyagi, A. K.; Drlica, K.; Singh, Y.; Ullrich, A. Cloning and Characterization of Secretory Tyrosine Phosphatases of *Mycobacterium tuberculosis*. *J. Bacteriol.* **2000**, *182*, 5425–5432.

(10) Koul, A.; Herget, T.; Klebl, B.; Ullrich, A. Interplay between mycobacteria and host signalling pathways. *Nature Rev. Microbiol.* **2004**, *2*, 189–202.

(11) Chao, J.; Wong, D.; Zheng, X.; Poirier, V.; Bach, H.; Hmama, Z.; Av-Gay, Y. Protein kinase and phosphatase signaling in *Mycobacterium tuberculosis* physiology and pathogenesis. *Biochim. Biophys. Acta* **2010**, *1804*, 620–627.

(12) Bach, H.; Papavinasasundaram, K. G.; Wong, D.; Hmama, Z.; Av-Gay, Y. *Mycobacterium tuberculosis* Virulence Is Mediated by PtpA Dephosphorylation of Human Vacuolar Protein Sorting 33B. *Cell Host Microbe* **2008**, *3* (5), 316–322.

(13) Bach, H.; Wong, D.; Av-Gay, Y. *Mycobacterium tuberculosis* PtkA is a novel protein tyrosine kinase whose substrate is PtpA. *Biochem. J.* **2009**, *420* (2), 155–160.

(14) Singh, R.; Rao, V.; Shakila, H.; Gupta, R.; Khera, A.; Dhar, N.; Singh, A.; Koul, A.; Singh, Y.; Naseema, M.; Narayanan, P. R.; Paramasivan, C. N.; Ramanathan, V. D.; Tyagi, A. K. Disruption of mptpB impairs the ability of *Mycobacterium tuberculosis* to survive in guinea pigs. *Mol. Microbiol.* **2003**, *50* (3), 751–762.

(15) Zhou, B.; He, Y.; Zhang, X.; Xu, J.; Luo, Y.; Wang, Y.; Franzblau, S. G.; Yang, Z.; Chan, R. J.; Liu, Y.; Zheng, J.; Zhang, Z. Y. Targeting mycobacterium protein tyrosine phosphatase B for antituberculosis agents. *Proc. Natl. Acad. Sci. U.S.A.* **2010**, *107* (10), 4573–4578.

(16) (a) Tabernero, L.; Aricescu, A. R.; Jones, E. Y.; Szedlacsek, S. E. Protein tyrosine phosphatases: structure–function relationships. *FEBS J.* **2008**, *275*, 867–882. (b) Zhang, Z. Y. Protein tyrosine phosphatases: prospects for therapeutics. *Curr. Opin. Chem. Biol.* **2001**, *5*, 416–423.

(17) Bialy, L.; Waldmann, H. Inhibitors of Protein Tyrosine Phosphatases: Next Generation Drugs? *Angew Chem. Int. Ed.* **2005**, *44* (25), 3814–3839.

(18) Vintonyak, V. V.; Antonchick, A. P.; Rauh, D.; Waldmann, H. The therapeutic potential of phosphatase inhibitors. *Curr. Opin. Chem. Biol.* **2009**, *13*, 272–283.

(19) Greenstein, A. E.; Grundner, C.; Echols, N.; Gay, L. M.; Lombana, T. N.; Miecskowski, C. A.; Pullen, K. E.; Sung, P. Y.; Alber, T. Structure/Function Studies of Ser/Thr and Tyr Protein Phosphorylation in *Mycobacterium tuberculosis*. *J. Mol. Microbiol. Biotechnol.* **2005**, *9*, 167–181.

(20) Manger, M.; Scheck, M.; Prinz, H.; Von Kries, J. P.; Langer, T.; Saxena, K.; Schwalbe, H.; Fürstner, A.; Rademann, J.; Waldmann, H. Discovery of *Mycobacterium Tuberculosis* Protein Tyrosine Phosphatase A (MptpA) Inhibitors Based on Natural Products and a Fragment-Based Approach. *ChemBioChem* **2005**, *6*, 1749–1753.

(21) Madhurantakam, C.; Chavali, V. R. M.; Das, K. A. Analyzing the catalytic mechanism of MPtpA: a low molecular weight protein tyrosine phosphatase from *Mycobacterium tuberculosis* through site-directed mutagenesis. *Proteins* **2008**, *71*, 706–714.

(22) Rawls, K. A.; Lang, P. T.; Takeuchi, J.; Imamura, S.; Baguley, T. D.; Grundner, C.; Alber, T.; Ellman, J. A. Fragment-based discovery of selective inhibitors of the *Mycobacterium tuberculosis* protein tyrosine phosphatase PtpA. *Bioorg. Med. Chem. Lett.* **2009**, *19*, 6851–6854.

(23) Grundner, C.; Perrin, D; Van Huijsduijnen, R. H.; Swinnen, D.; Gonzalez, J.; Gee, C. L.; Wells, T. N.; Alber, T. Structural Basis for Selective Inhibition of *Mycobacterium tuberculosis* Protein Tyrosine Phosphatase PtpB. *Structure* **2007**, *15* (4), 499–509.

(24) (a) Nören-Müller, A.; Reis-Corrêa, I. Jr.; Prinz, H.; Rosenbaum, C.; Saxena, K.; Schwalbe, H. J.; Vestweber, D.; Cagna, G.; Schunk, S.; Schwarz, O.; Schiewe, H.; Waldmann, H. Discovery of protein phosphatase inhibitor classes by biology-oriented synthesis. *Proc. Natl. Acad. Sci. U.S.A.* **2006**, *103* (28), 10606–10611. (b) Nören-Müller, A.; Wilk, W.; Saxena, K.; Schwalbe, H.; Kaiser, M.; Waldmann, H. Discovery of a New Class of Inhibitors of *Mycobacterium tuberculosis* Protein Tyrosine Phosphatase B by Biology-Oriented Synthesis. *Angew Chem. Int. Ed.* **2008**, *47*, 5973–5977. (c) Corrêa, I. R. Jr.; Nören-Müller, A.; Ambrosi, H. D.; Jakupovik, S.; Saxena, K.; Schwalbe, H.; Kaiser, M.; Waldmann, H. Identification of Inhibitors for Mycobacterial Protein Tyrosine Phosphatase B (MptpB) by Biology-Oriented Synthesis (BIOS). *Chem. Asian. J.* **2007**, *2*, 1109–1126.

(25) (a) Beresford, N. J.; Mulhearn, D.; Szczepankiewicz, B.; Liu, G.; Johnson, M. E.; Fordham-Skelton, A.; Abad-Zapatero, C.; Cavet, J. S.; Tabernero, L. Inhibition of MptpB phosphatase from *Mycobacterium tuberculosis* impairs mycobacterial survival in macrophages. *J. Antimicrob. Chemother.* **2009**, *63*, 928–936. (b) Soellner, M. B.; Rawls, K. A.; Grundner, C.; Alber, T.; Ellman, J. A. Fragment-Based Substrate Activity Screening Method for the Identification of Potent Inhibitors of the *Mycobacterium tuberculosis* Phosphatase PtpB. *J. Am. Chem. Soc.* **2007**, *129* (31), 9613–9615.

(26) (a) Vintonyak, V. V.; Warburg, K.; Over, B.; Hübel, K.; Rauh, D.; Waldmann, H. Identification and further development of thiazolidinones spiro-fused to indolin-2-ones as potent and selective inhibitors of *Mycobacterium tuberculosis* protein tyrosine phosphatase B. *Tetrahedron* **2011**, *67* (35), 6713–6729. (b) Oliveira, K. N.; Chiaradia, L. D.; Martins, P. G. A.; Mascarello, A.; Cordeiro, M. N.; Guido, R. V. C.; Andricopulo, A. D.; Yunes, R. A.; Nunes, R. J.; Vernal, J.; Terenzi, H. Sulfonyl-hydrazones of cyclic imides derivatives as potent inhibitors of the *Mycobacterium tuberculosis* protein tyrosine phosphatase B (PtpB). *MedChemComm* **2011**, *2*, 500–504.

(27) Chiaradia, L. D.; Mascarello, A.; Purificação, M.; Vernal, J.; Cordeiro, M. N. S.; Zenteno, M. E.; Villarino, A.; Nunes, R. J.; Yunes,

R. A.; Terenzi, H. Synthetic chalconas as efficient inhibitors of *Mycobacterium tuberculosis* protein tyrosine phosphatase PtpA. *Bioorg. Med. Chem. Lett.* **2008**, *18*, 6227−6230.

(28) Mascarello, A.; Chiaradia, L. D.; Vernal, J.; Villarino, A.; Guido, R. V. C.; Perizzolo, P.; Poirier, V.; Wong, D.; Martins, P. G. A.; Nunes, R. J.; Yunes, R. A.; Andricopulo, A. D.; Av-Gay, Y.; Terenzi, H. Inhibition of *Mycobacterium tuberculosis* tyrosine phosphatase PtpA by synthetic chalcones: Kinetics, molecular modeling, toxicity and effect on growth. *Bioorg. Med. Chem.* **2010**, *18*, 3783−3789.

(29) Yoon, G.; Lee, W.; Kim, S. N.; Cheon, S. H. Inhibitory effect of chalcones and their derivatives from *Glycyrrhiza inflata* on protein tyrosine phosphatase 1B. *Bioorg. Med. Chem. Lett.* **2009**, *19*, 5156−5157.

(30) Nayyar, A.; Jain, R. Recent advances in new structural classes of anti-tuberculosis agents. *Curr. Med. Chem.* **2005**, *12* (16), 1873−1886.

(31) Lin, Y. M.; Zhou, Y.; Flavin, M. T.; Zhow, L. M.; Nie, W.; Chen, F. C. Chalcones and Flavonoids as Anti-Tuberculosis Agents. *Bioorg. Med. Chem.* **2002**, *10* (8), 2795−2802.

(32) Sivakumar, P. M.; Seenivasan, S. P; Kumar, V.; Doble, M. Synthesis, antimycobacterial activity evaluation and QSAR studies of chalcone derivatives. *Bioorg. Med. Chem. Lett.* **2007**, *17*, 1695−1700.

(33) Hans, R. H.; Guantai, E. M.; Lategan, C.; Smith, P J.; Wan, B.; Franzblau, S. G.; Gut, J.; Rosenthal, P. J.; Chibale, K. Synthesis, antimalarial and antitubercular activity of acetylenic chalcones. *Bioorg. Med. Chem. Lett.* **2010**, *20*, 942−944.

(34) Tsai, S.; Klinmam, J. P. De novo design and utilization of photolabile caged substrates as probes of hydrogen tunneling with horse liver alcohol dehydrogenase at sub-zero temperatures: a cautionary note. *Bioorg. Chem.* **2003**, *31*, 172−190.

(35) Högberg, T.; Bengtsson, S.; Paulis, T.; de.; Johansson, L.; Ström, P; Hall, H.; Ögren, S. O. Potential antipsychotic agents 5—Synthesis and antidopaminergic properties of substituted 5,6-dimethoxysalicylamides and related compounds. *J. Med. Chem.* **1990**, *33* (4), 1155−1163.

(36) (a) Gulati, K. C.; Seth, S. R.; Venkataraman, K. Phloroacetophenone. *Org. Synth.* **1943**, *2*, 522. Gulati, K. C.; Seth, S. R.; Venkataraman, K. Phloroacetophenone. *Org. Synth.* **1935**, *15*, 70 http://www.orgsyn.org/orgsyn/prep.asp?prep=cv2p0522. (b) Chiaradia, L. D.; dos Santos, R.; Vitor, C. E.; Vieira, A. A.; Leal, P. C.; Nunes, R. J.; Calixto, J. B.; Yunes, R. A. Synthesis and pharmacological activity of chalcones derived from 2,4,6-trimethoxyacetophenone in RAW 264.7 cells stimulated by LPS: Quantitative structure−activity relationships. *Bioorg. Med. Chem.* **2008**, *16*, 658−667.

(37) (a) Topliss, J. G. Utilization of Operational Schemes for Analog Synthesis in Drug Design. *J. Med. Chem.* **1972**, *15*, 1006−1011. (b) Lipinski, C. A.; Lombardo, F.; Dominy, B. W.; Feeney, P. J. Experimental and computational approaches to estimate solubility and permeability in drug discovery and development settings. *Adv. Drug Delivery Rev.* **1997**, *23*, 3−25.

(38) (a) Insuasty, B.; Quiroga, J.; Abonia, R.; Insuasty, H.; Mosquera, M.; Cruz, S.; Nogueras, M.; Sortino, M.; Zacchino, S. Synthesis induced by microwave irradiation and in vitro antifungal evaluation of new dihydropyrazolo[3,4-*b*][1,4]diazepines. *Heterocycl. Commun.* **2004**, *10* (1), 103−108. (b) Sivakumar, P. M.; Priya, S.; Doble, M. Synthesis, Biological Evaluation, Mechanism of Action and Quantitative Structure−Activity Relationship Studies of Chalcones as Antibacterial Agents. *Chem. Biol. Drug Des.* **2009**, *73* (4), 403−415. (c) Ishii, H.; Ishikawa, T.; Deushi, T.; Harada, K.; Watanabe, T.; Ueda, E.; Ishida, T.; Sakamoto, M.; Kawanabe, E.; Takahashi, T.; Ichikawa, Y. I.; Takizawa, K.; Masuda, T.; Chen, I. S. Studies on the chemical constituents of Rutaceous plants. XLIX. Development of a versatile method for the synthesis of antitumor-active benzo[*c*]phenanthridine alkaloids. (1). Preparation of various 2,4-bisaryl-4-oxo-butyronitriles and 2,4-bisaryl-4-oxobutyramides. *Chem. Pharm. Bull.* **1983**, *31* (9), 3024−3038. (d) Janka, M.; He, W.; Frontier, A. J.; Flaschenriem, C.; Eisenberg, R. Preorganization in the Nazarov cyclization: the role of adjacent coordination sites in the highly Lewis acidic catalyst $[IrMe(CO)(dppe)(DIB)](Bar^f_4)_2$. *Tetrahedron* **2005**, *61*, 6193−6206. (e) Wattanasin, S.; Murphy, W. S. An improved procedure for the preparation of chalcones and related enones. *Synthesis* **1980**, *8*, 647−650. (f) Insuasty, B.; Orozco, F.; Quiroga, J.; Abonia, R.; Nogueras, M.; Cobo, J. Microwave induced synthesis of novel 8,9-dihydro-7*H*-pyrimido[4,5-*b*][1,4]diazepines as potential antitumor agents. *Eur. J. Med. Chem.* **2008**, *43* (9), 1955−1962. (g) Sadashivamurthy, B.; Basavaraju, Y. B. New tetralone esters as intermediates for the synthesis of podophyllotoxin analogs. *Indian J. Heterocycl. Chem.* **2006**, *15* (3), 259−262. (h) Satisha, A. D.; Hemakumar, K. H.; Basavaraju, Y. B. Synthesis of new tetralone ester intermediates for podophyllotoxin analogues. *Indian J. Heterocycl. Chem.* **2007**, *17* (1), 15−18. (i) Xia, Y.; Yang, Z. Y.; Xia, P.; Bastow, K. F.; Nakanishi, Y.; Lee, K. H. Antitumor Agents. Part 202: Novel 2′-Amino Chalcones: Design, Synthesis and Biological Evaluation. *Bioorg. Med. Chem. Lett.* **2000**, *10* (8), 699−701. (j) Jung, J. C.; Jang, S.; Lee, Y.; Min, D.; Lim, E.; Jung, H.; Oh, M.; Oh, S.; Jung, M. Efficient Synthesis and Neuroprotective Effect of Substituted 1,3-Diphenyl-2-ppropen-1-ones. *J. Med. Chem.* **2008**, *51* (13), 4054−4058. (k) Parmar, V. S.; Sharma, S.; Rathore, J. S.; Garg, M.; Gupta, S.; Malhotra, S.; Sharma, V. K.; Singh, S.; Boll, P. M. Carbon-13 nuclear magnetic resonance studies on 1,3-diphenylprop-2-enones. *Magn. Reson. Chem.* **1990**, *28* (5), 470−474. (l) Ariyan, Z. S.; Suschitzky, H. Heterocyclic compounds of the chalcone type. *J. Chem. Soc., Abstr.* **1961**, 2242−2244. (m) Anjaneyulu, A. S. R.; Rani, G. S.; Mallavadhani, U. V.; Murthy, Y. L. N. Synthesis and characterization of some new chalcones and flavanones. *Indian J. Heterocycl. Chem.* **1994**, *4* (1), 9−14. (n) Thirunarayanan, G. Effects of substituent on 1H and 13C NMR chemical shifts in substituted styryl 2-naphthyl ketones. *Acta Cienc. Indica, Chem.* **2003**, *29* (3), 147−150. (o) Lubisch, W.; Moeller, A.; Treiber, H. J. Preparation of *N*-(2-oxoethyl)benzamides as cysteine protease inhibitors. *Ger. Offen* **1998**, 34 pp. (p) Wagner, G.; Voigt, B.; Daenicke, D.; Liebermann, T. Synthesis of 1-aryl-3-[amidinophenyl]-propanones-(1) and other derivatives with a carbonyl group in γ-position to the amidinophenyl radical. *Pharmazie* **1976**, *31* (8), 528−532. (q) Levai, A.; Jozsef, J. Synthesis of 1-substituted 3,5-diaryl-2-pyrazolines by the reaction of α,β -unsaturated ketones with hydrazines. *J. Heterocycl. Chem.* **2006**, *43* (1), 111−115. (r) Gutteridge, C. E.; Vo, J. V.; Tillett, C. B.; Vigilante, J. A.; Dettmer, J. R.; Patterson, S. L.; Werbovetz, K. A.; Capers, J.; Nichols, D. A.; Bhattacharjee, A. K.; Gerena, L. Antileishmanial and Antimalarial Chalcones: Synthesis, Efficacy and Cytotoxicity of Pyridinyl and Naphthalenyl Analogs. *Med. Chem.* **2007**, *3* (2), 115−119. (s) Regaila, H. A. A. Synthesis of newer *N*-acetyl-, *N*-arylpyrazoline, -isoxazole, and -benzodioxane derivatives of biological activity. *Egypt J. Pharm. Sci.* **1988**, *29* (1−4), 191−206.

(39) (a) Borchhardt, D. M.; Mascarello, A.; Chiaradia, L. D.; Nunes, R. J.; Oliva, G.; Yunes, R. A.; Andricopulo, A. D. Biochemical Evaluation of a Series of Synthetic Chalcone and Hydrazide Derivatives as Novel Inhibitors of Cruzain from *Trypanosoma cruzi*. *J. Braz. Chem. Soc.* **2010**, *21* (1), 142−150. (b) Winter, E.; Chiaradia, L. D.; Cordova, C. A. S; de; Nunes, R. J.; Yunes, R. A.; Creczynski-Pasa, T. B. Naphthylchalcones induce apoptosis and caspase activation in a leukemia cell line: The relationship between mitochondrial damage, oxidative stress and cell death. *Bioorg. Med. Chem.* **2010**, *18*, 8026−8034. (c) Alberton, E. H.; Damazio, R. G.; Cazarolli, L. H.; Chiaradia, L. D.; Leal, P. C.; Nunes, R. J.; Yunes, R. A.; Silva, F. R. B. S. Influence of chalcone analogues on serum glucose levels in hyperglycemic rats. *Chem. Biol. Interact.* **2008**, *171*, 355−362. (d) Pedrini, F. S.; Chiaradia, L. D.; Licínio, M. A.; Moraes, A. C. R.; de; Curta, J. C.; Costa, A.; Mascarello, A.; Creczynski-Pasa, T. B.; Nunes, R. J.; Yunes, R. A.; Santos-Silva, M. C. Induction of apoptosis and cell cycle arrest in L-1210 murine lymphoblastic leukaemia cells by (2*E*)-3-(2-naphthyl)-1-(3′-methoxy-4′-hydroxy-phenyl)-2-propen-1-one. *J. Pharm. Pharmacol.* **2010**, *62*, 1128−1136.

(40) Postigo, M. P.; Krogh, R.; Terni, M. F.; Pereira, H. M.; Oliva, G.; Castilho, M. S.; Andricopulo, A. D. Enzyme kinetics, structural analysis and molecular modeling studies on a series of *Schistosoma mansoni* PNP inhibitors. *J. Braz. Chem. Soc.* **2011**, *22*, 583−591.

(41) (a) Postigo, M. P.; Guido, R. V.; Oliva, G.; Castilho, M. S.; da R. Pitta, I.; de Albuquerque, J. F.; Andricopulo, A. D. Discovery of new inhibitors of *Schistosoma mansoni* PNP by pharmacophore-based

virtual screening. *J. Chem. Inf. Model.* **2010**, *50*, 1693−1705. (b) Severino, R. P.; Guido, R. V.; Marques, E. F.; Brömme, D.; da Silva, M. F.; Fernandes, J. B.; Andricopulo, A. D.; Vieira, P. C. Acridone alkaloids as potent inhibitors of cathepsin V. *Bioorg. Med. Chem.* **2011**, *19*, 1477−1481.

(42) Guo, X. L.; Shen, K.; Wang, F.; Lawrence, D. S.; Zhang, Z. Y. Probing the Molecular Basis for Potent and Selective Protein−tyrosine Phosphatase 1B Inhibition. *J. Biol. Chem.* **2002**, *227*, 41014−41022.

(43) Copeland, R. A. Reversible Modes of Inhibitor Interactions with Enzymes. In *Evaluation of Enzyme Inhibitors in Drug Discovery*; Wiley Interscience: Hoboken, NJ, 2005; pp 48−81.

(44) (a) Ferreira, R. S.; Guido, R. V. C.; Andricopulo, A. D.; Oliva, G. In Silico Screening Strategies for Novel Inhibitors of Parasitic Diseases. *Expert Opin. Drug. Discovery* **2011**, *6* (5), 481−489. (b) Guido, R. V. C.; Oliva, G.; Andricopulo, A. D. Virtual Screening and Its Integration with Modern Drug Design Technologies. *Curr. Med. Chem.* **2008**, *15*, 37−46. (c) Andricopulo, A. D.; Salum, L. B.; Abraham, D. J. Structure-Based Drug Design Strategies In Medicinal Chemistry. *Curr. Top. Med. Chem.* **2009**, *9* (9), 771−790. (d) Guido, R. V. C.; Oliva, G. Structure-Based Drug Discovery for Tropical Diseases. *Curr. Top. Med. Chem.* **2009**, *9* (9), 824−843.

(45) Supplementary informationof Ecco, G.; Vernal, J.; Razzera, G.; Martins, P. G.; Matiollo, C.; Terenzi, H. *Mycobacterium tuberculosis* tyrosine phosphatase A (PtpA) activity is modulated by *S*-nitrosylation. *Chem. Commun.* **2010**, *46* (40), 7501−7503.

(46) (a) Porath, J. Immobilized metal ion affinity chromatography. *Protein Expression Purif.* **1992**, *3* (4), 263−281. (b) Martins, S.; Farnaud, S.; Pacheco, V.; Pacheco, R.; Karmali, A.; Tata, R.; Brown, P. R. Differential behavior of recombinant wild-type and altered amidases on immobilized metal-ion affinity chromatography. *Int. J. Bio-Chromatogr.* **2000**, *5* (2), 111−129.

(47) Bradford, M. M. A rapid and sensitive method for the quantitation of microgram quantities of protein utilizing the principle of protein−dye binding. *Anal. Biochem.* **1976**, *72* (1−2), 248−254.

(48) Barford, D.; Flint, A. J.; Tonks, N. K. Crystal Structure of Human Protein Tyrosine Phosphatase 1B. *Science* **1994**, *263* (5152), 1397−1404.

(49) Clark, M.; Cramer, R. D.; van Opdenbosch, N. Validation of the general purpose tripos 5.2 force Field. *J. Comput. Chem.* **1989**, *10*, 982−1012.

(50) Powell, M. J. D. Restart procedures for the conjugate gradient method. *Math. Program* **1977**, *12*, 241−254.

(51) Gasteiger, J.; Marsili, M. Iterative partial equalization of orbital electronegativity—a rapid access to atomic charges. *Tetrahedron* **1980**, *36*, 3219−3228.

(52) Jones, G.; Willett, P.; Glen, R. C.; Leach, A. R.; Taylor, R. D. Development and Validation of a Genetic Algorithm for Flexible Docking. *J. Mol. Biol.* **1997**, *267*, 727−748.